WBS 1.3.4 – Heat and Radiation Shield Reference Design

Document No:	Created:	12/30/2002	Page: 1 of 20
MECO-TGT-02-001	Modified:	1/22/04	Version: 1.07

Prepared by:

M. Hebert, V. Tumakov

Revised by:

M. Hebert, V. Tumakov, W. Molzon, B. Christensen

Approved by:

QA Officer (TBD)

Abstract

This document contains the parameters defining the Heat and Radiation Shield that serves to protect the superconducting coils of the Production Solenoid from the heat and ionizing radiation generated by the primary proton beam striking the production target. This document includes mechanical properties of the system as well as estimates of the energy deposition and accumulated dose in the PS coils with this shield configuration operating at the nominal proton beam intensity.

History of Changes

Rev. No.	Date	Sections	Description of changes
1.00	12/30/02	All	Initial version containing a few mechanical parameters and some 3D CAD modeling sketches.
1.01	1/06/03	All	Additional tungsten insert adjacent to target extending from 25 cm to 30 cm radially to reduce maximum instantaneous heating there. Thinned shield near proton exit to reduce (if not eliminate) beam scraping.
1.02	1/24/03	All	Replaced plate insert with cylindrical tungsten shell. Added mandrel and He can energy deposition to cold mass total.
1.03	2/6/03	3	Corrected PHC4 mass and added COG data for all volumes.
1.04	9/4/03	All	Added P3CL insert at interface with TSu to shield TS coils. Added estimates of beam heating in shield materials. Upped coil energy deposition limit to 25 μW/g. Added MIT CDR design ideas. Redefined role of PSTB.
1.05	9/18/03	All	PS coil build changes required update of energy deposition. Filled gap between shield and PS cryostat at TS end for structural reasons. Revised beam aperture to conical shape for relief in beam fault conditions and addition space within TS cryostat. Added UCI design concept drawings.
1.06	10/30/03	3	Revised PBEM aperture numbers, adding positions of upstream and downstream centers in the MECO coordinate system. Adjusted position of P3CL.
1.07	1/22/04	3	Revised dimensions and positions of PHC1, P3CL, PCLG. Also changed proton beam aperture PBEM to an elliptical cross-section per MECO Memo 114, repositioned per current simulations. Did NOT update overview drawings.

Table of Contents

1. INTRODUCTION 4

2. REQUIREMENTS 4

2.1 Maximum Instantaneous Power Dissipation At Any Position Within the Production Solenoid Coils 4
2.2 Maximum Total Power Dissipation Within the Production Solenoid Cold Mass 5
2.3 Minimum Clear Bore 5
2.4 Heat Removal 5
2.5 Operation within a Vacuum 5
2.6 Operation in a High Radiation Environment 5
2.7 Pointing Geometry 5

3. DESIGN 5

3.1 Component Volumes from the Physics Simulation 5
3.2 Cooling 8
3.3 Ring Stiffeners 9
3.4 Pre-conceptual Design 9
3.5 Installation and Removal After Activation 14

4. INTERFACES 14

4.1 Allowed envelope 14
4.2 Fluid 15

5. EXPECTED PERFORMANCE 15

5.1 Estimated Radiation Load On PS Coils 15
5.2 Expected Activation 19

6. REFERENCES 20

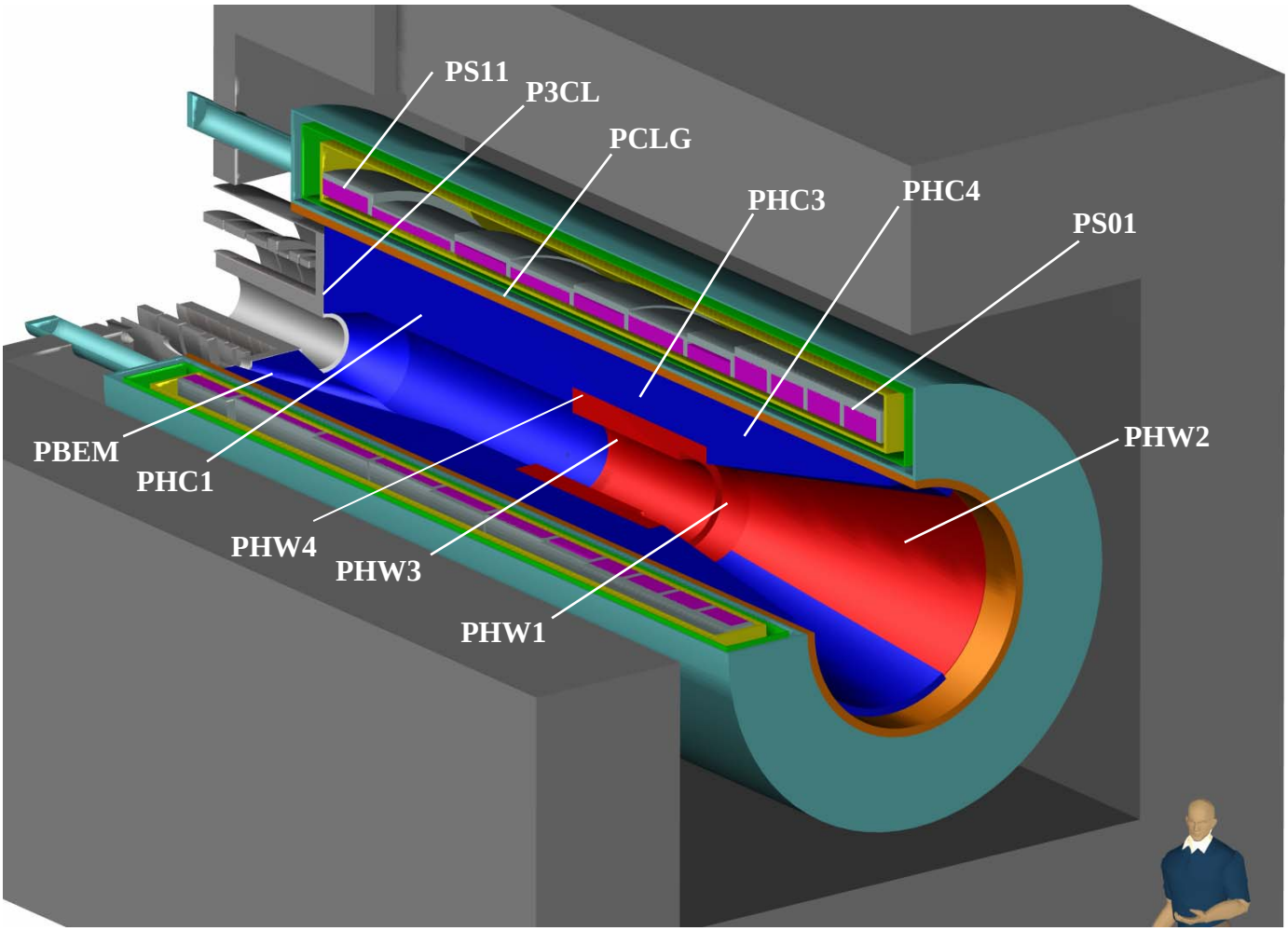

Figure 1.1 – Cutaway view of the Heat and Radiation Shield (WBS 1.3.4) within the warm bore of the Production Solenoid. In the figure, copper is blue and tungsten is red, while the stainless steel volumes are in several colors to distinguish regions. The separate volumes that together form the copper and tungsten regions are illustrated in Figure 3.1.

1. INTRODUCTION

This document describes the Heat and Radiation Shield (WBS 1.3.2) that serves to protect the superconducting coils of the Production Solenoid (PS) from the ionizing radiation generated by the primary proton beam striking the production target within the warm bore of the PS. At present the design consists of a series of simple three-dimensional volumes described below. These volumes are used in the physics simulation (GEANT3) to measure the effect of variations in material choices and dimensions. A cut-away illustration of the heat shield and PS is shown in Figure 1.1. The upstream elements of the Transport Solenoid (TS) including the first collimator are shown in grey in their positions immediately downstream of the heat shield in the figure.

2. REQUIREMENTS

2.1 Maximum Instantaneous Power Dissipation At Any Position Within the Production Solenoid Coils

The shield shall limit the instantaneous local heating in the Production Solenoid coils due to radiation originating in the production target to less than 25 μW/gm at any point within the coil volume.

2.2 Maximum Total Power Dissipation Within the Production Solenoid Cold Mass

The shield shall limit the total steady-state power dissipation in the cold mass of the Production Solenoid to less than 150 W.

2.3 Minimum Clear Bore

GEANT simulations [1] indicate that the inner radius of the shield must be greater than or equal to 25 cm to maintain the required muon stopping rate per incident proton.

2.4 Heat Removal

The shield shall be actively cooled to remove ~16 kW of heat generated within its volume by radiation from the production target.

2.5 Operation within a Vacuum

In the current design the vacuum boundary for the production region is at the PS cryostat inner wall, which places all elements of the heat shield within the production region vacuum.

2.6 Operation in a High Radiation Environment

By design the shield receives extremely high doses of radiation in order to prevent the PS coils from bearing that burden. As a result any materials used in the shield must be able to survive large (*how large?*) radiation doses without degrading to the point of failure. This includes any vacuum or fluid gasket materials or special low friction bearing surface materials.

2.7 Pointing Geometry

The assembled shield shall have no line-of-sight cracks from any point in the production target to any point in the PS cold mass.

3. DESIGN

3.1 Component Volumes from the Physics Simulation

At present the mechanical design of the shield is limited to a combination of copper and tungsten volumes (Figure 3.1) used in the physics simulation to optimise the shape and positioning of the shield components. The volumes that comprise the shield are described in the MECO Standard Coordinate System (MECO-Standards-03-001). **Dimensions are given in cm and angles are in degrees.** The volume names from the simulation code are given in parentheses.

Cylinder (PHC1)

Position of Center	Inner Radius	Outer Radius	Length	Material
(390.4, 0.0, -510.85)	30.0	70.0	234.1	Cu

Cylinder Section (PHC3)

Position of Center of Rotation	Inner Radius	Outer Radius	Length	Angular Range	Material
(390.4, 0.0, -690.4)	40.0	70.0	125.0	(-125.0, 130.0)	Cu

Conic Section (PHC4)

Position of Center of Rotation	Inner Rad. @ +z end	Inner Rad. @ -z end	Outer Radius	Length	Angular Range	Material
(390.4, 0.0, -837.9)	30.0	65.0	70.0	170.0	(-125.0, 130.0)	Cu

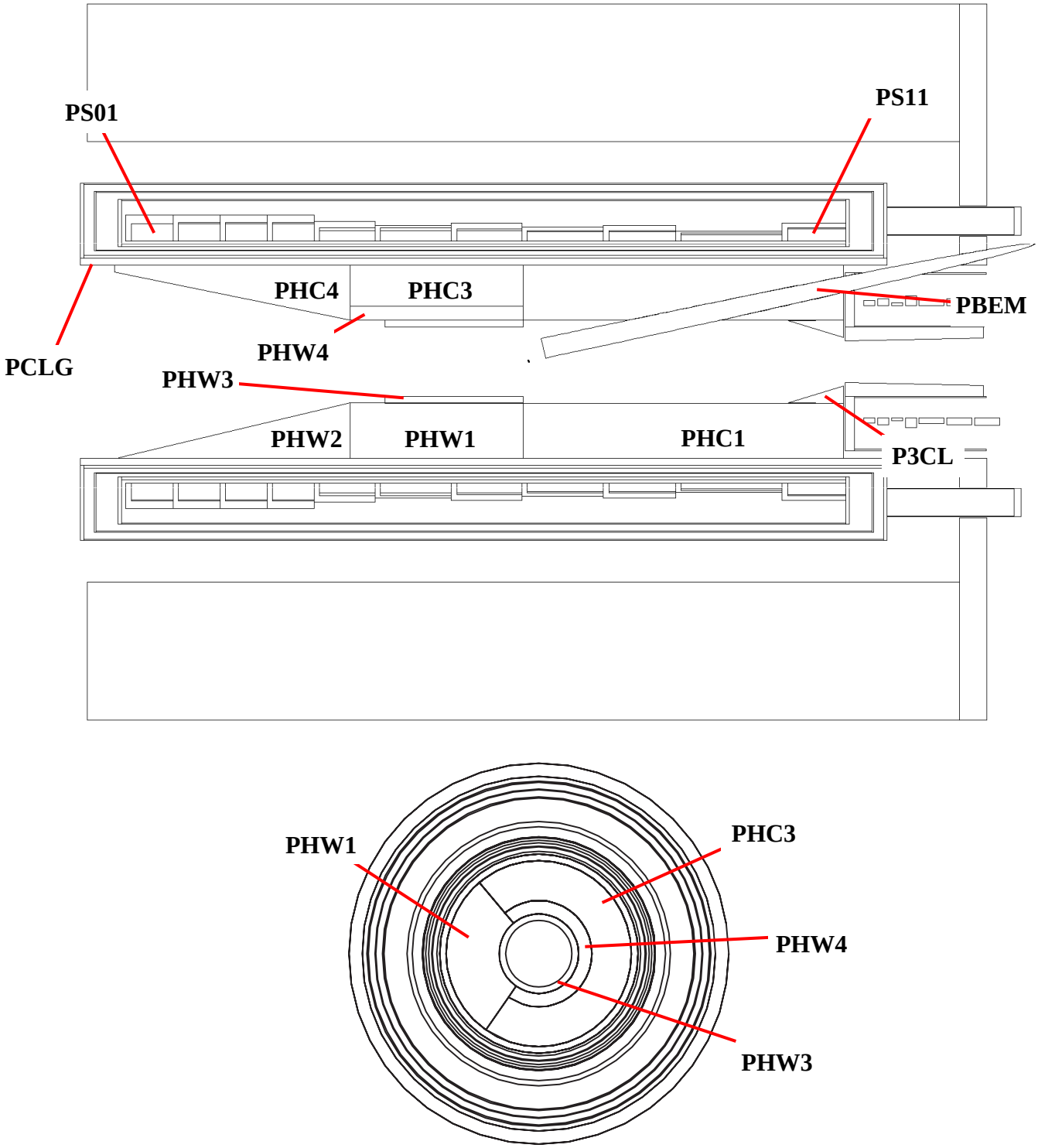

Figure 3.1 – Cross-section overhead and end (as seen from the Transport Solenoid) views of the Production Solenoid in the GEANT simulation showing the positions of the heat shield volumes.

Cylinder Section (PHW1)

Position of Center of Rotation	Inner Radius	Outer Radius	Length	Angular Range	Material
(390.4, 0.0, -690.4)	30.0	70.0	125.0	(130.0, 235.0)	W

Conic Section (PHW2)

Position of Center of Rotation	Inner Rad. @ +z end	Inner Rad. @ -z end	Outer Radius	Length	Angular Range	Material
(390.4, 0.0, -836.4)	30.0	69.5	70.0	167.0	(130.0, 235.0)	W

Cylinder (PHW3)

Position of Center	Inner Radius	Outer Radius	Length	Material
(390.4, 0.0, -677.9)	25.0	30.0	100.0	W

Cylinder Section (PHW4)

Position of Center of Rotation	Inner Radius	Outer Radius	Length	Angular Range	Material
(390.4, 0.0, -690.4)	30.0	40.0	125.0	(-125.0,130.0)	W

Conic Section (P3CL)

Position of Center of Rotation	Inner Rad. @ +z end	Inner Rad. @ -z end	Outer Radius	Length	Material
(390.4, 0.0, -414.8)	15.0	29.9	30.0	42.0	Cu

Cylinder (PCLG)

This volume consists of eight axial beams containing cooling channels and copper or brass shielding in between. For GEANT this is approximated as simply a copper cylinder

Position of Center	Inner Radius	Outer Radius	Length	Material
(390.4, 0.0, -670.72)	70.0	75.0	553.84	Cu

Proton Beam Aperture through the Heat Shield (PBEM)

This represents the evacuated elliptical passage (i.e. material removed) for the primary beam through the heat shield volumes. The rotations are performed in the order listed (i.e. about +y first, then about the new +x).

Position of Center	Horizontal Dia.	Vertical Dia.	Length	Rotation About +y	Rotation About +x	Material
(433.65, 0.25, -462.68)	14.0	18.0	416.0	12.032	1.277	Vacuum

For convenience, the positions of each end of the pipe after both rotations are given below in the nominal MECO coordinate system

Position of -Z End Center	Position of +Z End Center
(477.00, -4.38, -259.30)	(390.30, 4.89, -666.06)

Next version should include the small axial beam stop downstream of the production target as that will have to hang off the shield's inner radius.

Table 3.1 – Estimated masses of each of the shield components used in the physics simulation

Volume Name	Mass (metric tons)	Center of Gravity (cm)
PHC1	25.9	(390.3, 0.0, -512.4)
PHC3	8.2	(410.6, 0.88, -690.4)
PHC4	8.6	(411.1, 0.91, -819.4)
PHW1	8.8	(344.9, -1.99, -690.4)
PHW2	6.8	(340.1, -2.20, -812.6)
PHW3	1.7	(390.4, 0.0, -677.9)
PHW4	3.8	(403, 0.55, -690.4)
PCLG	11.9	(390.4, 0.0, -670.57)
P3CL	0.4	(390.4, 0.0, -416)
Total	**76.1**	(385.8, -0.2, -650.5)

3.2 Cooling

With the nominal beam {ref} on target, approximately 16 kW of heat is generated within the volumes of the Heat Shield by the passage of radiation. Nearly half (~6.2 kW) is generated within the PHW3 (see Figure 3.1) volume, i.e. the tungsten insert at the smallest radius near the production target. Table 3.2 lists the steady state radiation heat load in each section of the shield. In the table, the volume PCIW represents the inner wall of the PS cryostat as defined in MIT's Conceptual Design Report, while the PSTB volume (as defined above) represents the additional material needed for strengthening the wall to support the heat shield.

Table 3.2 – Estimated steady state radiation heat loads in sections of the heat shield identified by their GEANT names.

Volume Name	Power (W)	Volume Name	Power (W)	Volume Name	Power (W)
PHC1	1200	**PHW2**	1500	**PCLG**	300
PHC3	720	**PHW3**	6200	**PCIW**	41
PHC4	1000	**PHW4**	2000		
PHW1	2700	**P3CL**	80	**TOTAL**	**15741**

3.3 Ring Stiffeners

The inner shell of the PS cryostat is a large deep beam, and can support the weight of the shield, during insertion, and operation, if the loads are distributed well to the shell, and the shell is held round at several points along the length. To achieve this a series of annular ring stiffeners must be incorporated into the shield's structure. The exact number of annular plates remains TBD, but the concept is illustrated with five rings positioned at the ends and three intermediate points in Figure 3.2 below. The concept includes a radiation damage resistant bearing material (possibly Dicronite) on the outer edge of each ring to facilitate installation.

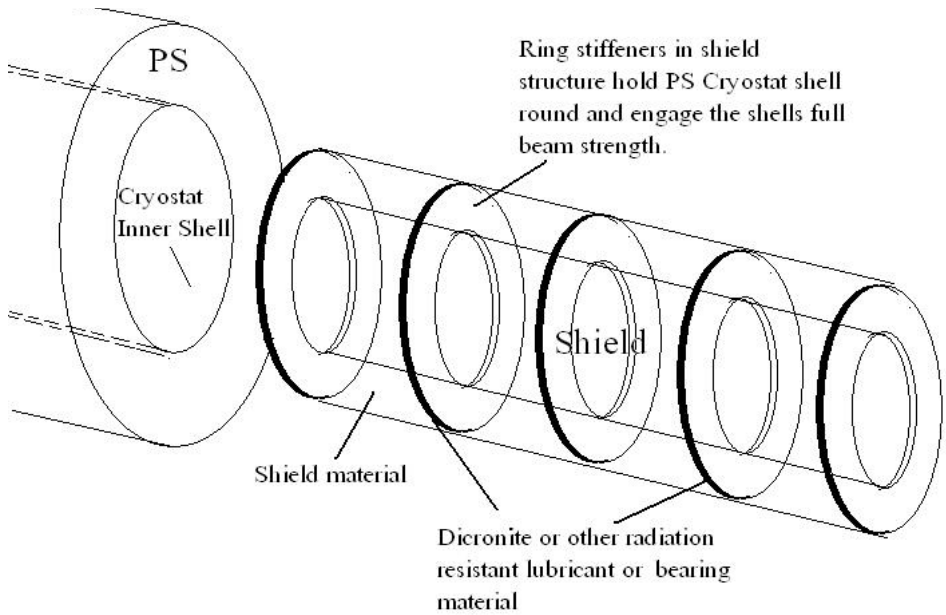

Figure 3.2 – An illustration of the use of ring stiffeners to engage the PS cryostat inner wall around its entire circumference to maximize the strength of the beam formed by the cryostat wall.

3.4 Pre-conceptual Design

The volumes that make up the heat and radiation shield in the simulation are too large to be easily managed or machined. In an attempt to make the construction more feasible a design concept has been proposed which will make the weight of each piece approximately 200 lbs. A method of actively cooling the heat shield has also been included with the goal of keeping the radial temperature change down to around 40 K. This design is only a basic sketch and the following numbers are the ones that were used in constructing the models. They do not necessarily reflect requirements.

The intended design is to make slices perpendicular to the z-axis, forming a ring as shown in Figure 3.3. Each ring could be made of 16 trapezoidal pieces. Alternate rings along the z-axis are left-to-right mirror images of one another, allowing for axial bolting between layers. This mirroring also prevents line of sight cracks down the length of the shield. Each copper piece is 12 cm thick axially while the tungsten sections are only 6 cm thick in order to meet the weight requirement (see Table 3.3). The tungsten sections are also of smaller outer radius (70 cm) than the copper sections (75 cm). The remaining 5 cm in the tungsten sections are filled with copper plates as a weight and cost saving measure.

Eight stainless steel beams will run the full length of the PS cryostat with ring stiffeners spaced along the length to maintain the circularity of the inner cryostat wall as per Section 3.3 above. Each of these beams will contain two 1 cm diameter water channels, one for supply and one for return, running the length of the beam. The channels will be internally joined at the TS end of the beam so that each beam forms a closed coolant loop with both inlet and outlet at the downstream end of the PS. This allows all soft connections to be made outside of the vacuum volume. The beams serve to cool the ring pieces via conduction. These beams will be

approximately 8 cm wide and 5 cm thick. The ring sections will be bolted to these beams for support and to improve heat transfer. The ring stiffeners are 3 cm thick and have an outer radius of 75 cm to reach the cryostat and an inner radius of 30 cm along the warm bore. As shown in Figure 3.5, there are 3 groups of 10 rings that make up the lowest radius section plus an additional 14 rings that make up the conical section, each section bounded by ring stiffeners. There is an additional stiffener ring on each end of the heat shield. These end rings are much thinner radially, but much longer axially to provide the required strength. For the proton beam exit side the end ring thickness must be minimized to prevent beam scraping, while on the TS end of the shield it must be thin to avoid conflicting with the TS outer cryostat wall.

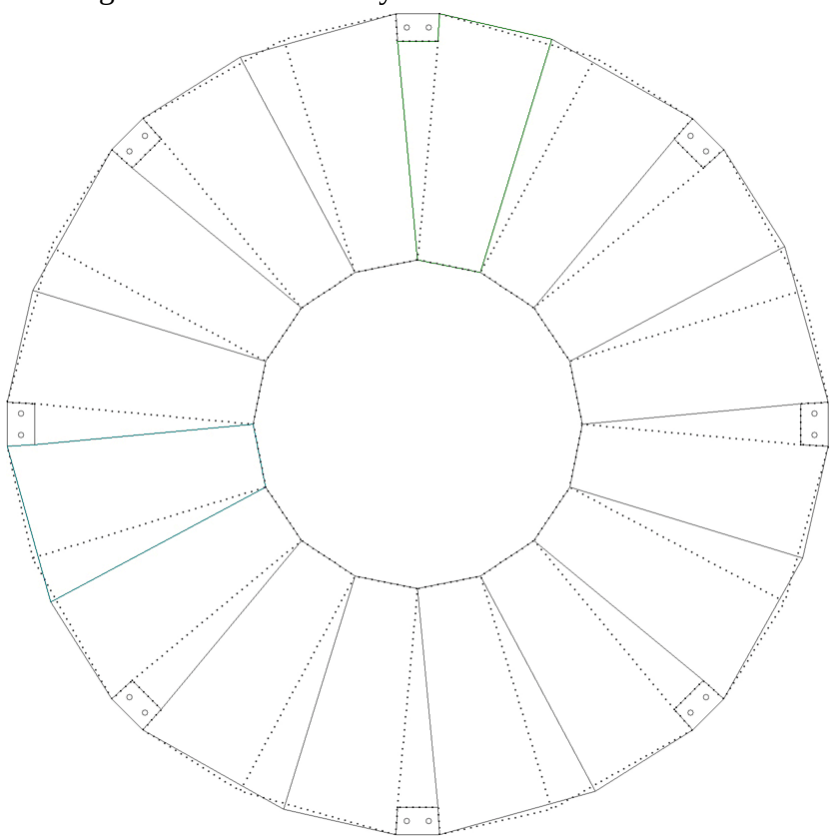

Figure 3.3 – An end view of two rings of the heat shield. The solid lines show the front ring of pieces. The following ring is a left to right mirror image of the front ring, shown in dotted lines. Both rings are made of only two types of pieces, the simple blue shape and the shape in green with a notch to accommodate the cooling beam.

Table 3.3 – Volumes and weights of the ring sections as shown in Figure 3.3.

	Volume (cm^3)	Material Density (g/cm^3)	Mass (kg)	Weight (lbs)
Blue Section (Cu)	1.06E+04	8.96	94.82	209.04
Green Section (Cu)	1.05E+04	8.96	93.74	206.65
Tungsten Section	4.43E+03	19.3	85.50	188.50

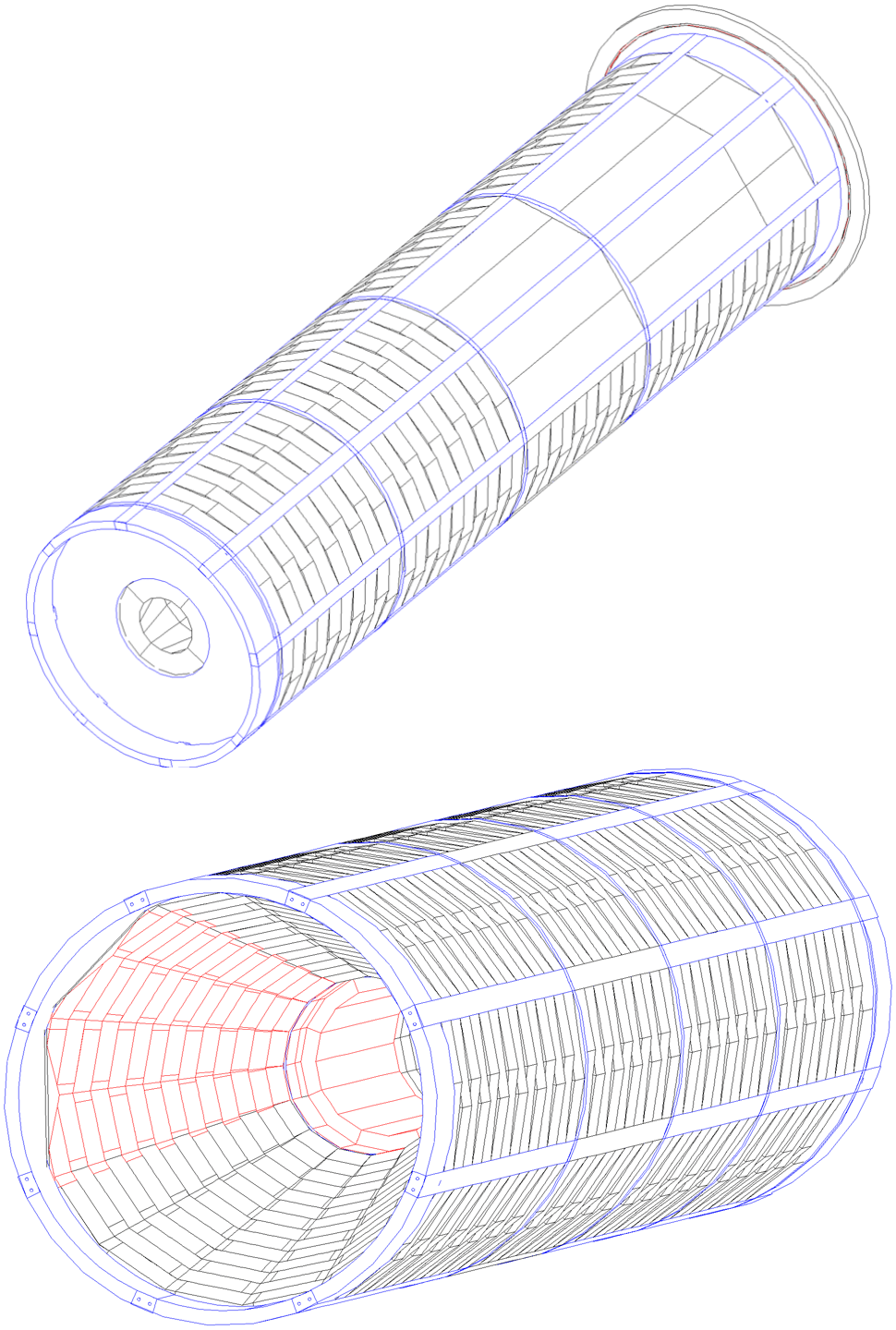

Figure 3.4 – Perspective views of the proposed heat shield design. The blue beams run the length of the cryostat and cool the ring sections. The blue ring stiffeners provide stability and circularity. The flat areas on the outside of the downstream end are copper plates that cover the tungsten sections. The red sections are made of tungsten.

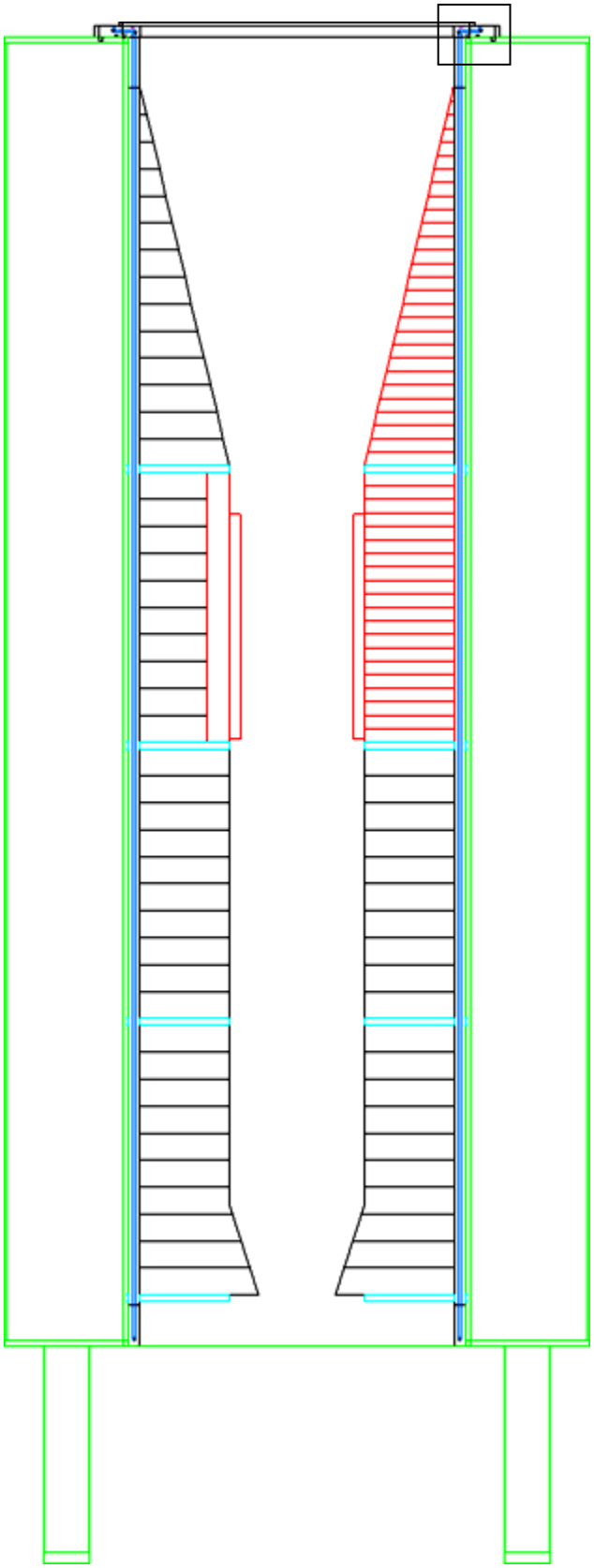

Figure 3.5 - Cross section of the heat shield. The tungsten ring sections (red) are half as thick as the copper sections. The highlighted region on the proton beam exit side is shown in detail in Figure 3.6.

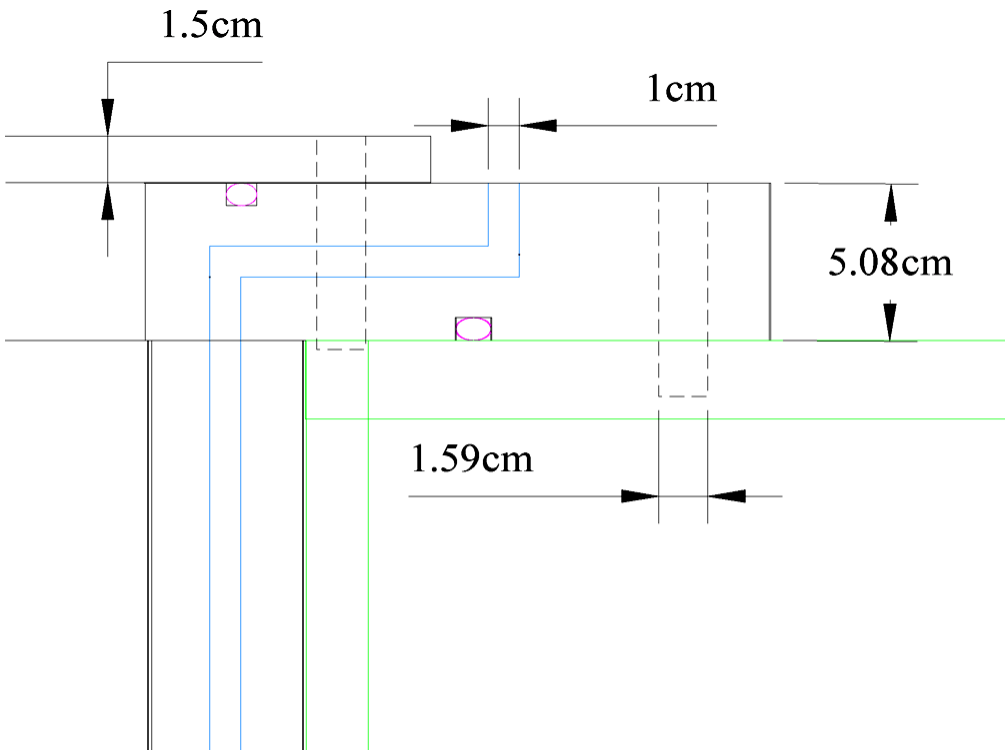

Figure 3.6 - Zoom of the indicated region in Figure 3.5. The blue lines define the water channel. The dashed lines show 5/8" boltholes for attaching the endplate to the cryostat.

The water pipes from the cooling beams exit through the downstream endplate as shown in Figure 3.6. The inlet and outlet are parallel and obscure each other in this view but are separated by 4 cm from center to center. All connections along the water channel will be welded to prevent leaks inside the vacuum volume. Soft connections will only begin at the outer ports shown in the close up.

The radial heat difference can be approximated using the heat flow equation $Q \approx k\Delta T \frac{A}{l}$. Approximately one third (110°) of each ring section immediately around the target is constructed of tungsten. The heat deposited in this azimuthal area along a one-meter section of the warm bore around the target is roughly 7000 W. This power is developed in a volume made up of about 18 tungsten ring sections, each with 4 pieces, making the power per piece (Q) equal to 97.2 W. If we assume the heat is deposited in the piece two-thirds of the distance in from the outer radius of the heat shield (as an approximation to the shower maximum location), the path length (l) from the hottest area to the cooling beam is about 30 cm. The cross-sectional area through which heat is conducted can be taken as the width of the piece at the inner radius (.117 m) times the depth of the piece (.06 m), giving an area A = .00702 m^2. Assuming the thermal conductivity of the tungsten alloy (k) is 120 W/m/K we calculate:

$$\Delta T = \frac{l}{A}\frac{Q}{k} = \frac{.30\ \text{m}}{.00702\ \text{m}^2}\frac{97.2\ \text{W}}{120\ \frac{\text{W}}{\text{m}\bullet\text{K}}} = 34.6\ \text{K}$$

The flow rate required through the beams to maintain a temperature difference of 5 K between the inlet and outlet temperatures can be calculated with a few assumptions. About 16 kW of heat load must be removed from the shield assembly by eight cooling beams. Because the heating is non-uniform we can estimate that one beam might have to absorb up to 4 kW of the heat.

$$m = \frac{Q}{c\Delta T} = \frac{4000\ \text{W}}{4.19\ \frac{\text{J}}{\text{g}\bullet\text{K}}\bullet 5\ \text{K}} = 190\,\frac{g}{s}$$

Max Temp Drop (K)	Heat (W)	Specific Heat (J/g/K)	Density (g/liter)
5	4000	4.186	1000

Mass Needed per time (g/s)
190

Flow Rates	
0.19	liters/sec
11.4	liters/min
3.0	**gallons/min**

Thus maintaining a 5 K inlet to outlet temperature difference requires about 3 gallons of water per minute to remove the anticipated shield heat load.

3.5 Installation and Removal After Activation

Requires a plan for installation including any special fixtures and a plan for minimizing personnel exposure during dismantling and removal. The large weight of the combined system exceeds the overhead crane limit of 40 tons, making installation more challenging. During the conceptual design effort for the solenoids, MIT put forth a sketch of one possible approach {ref} using temporary roller assemblies, that is duplicated here as Figure 3.7 for convenience. The rollers could be assisted with the overhead crane to reduce the insertion force and the resulting stresses on the PS cryostat. *We will need an estimate of the insertion force during installation including the increase in force if the cryostat inner wall is out-of-round.*

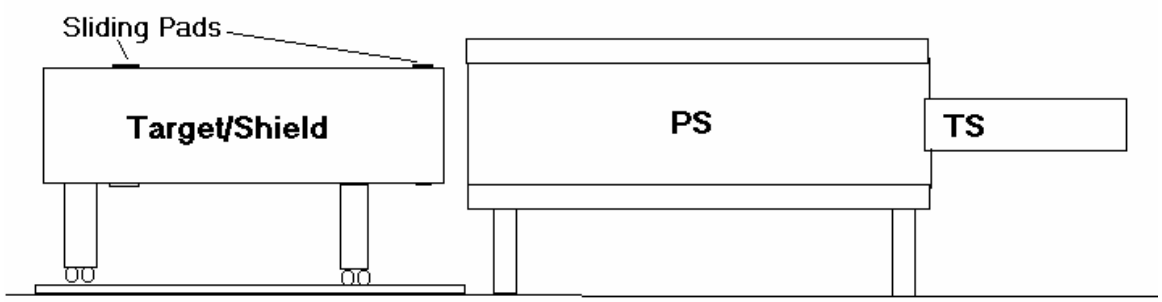

Figure 3.7 – A schematic illustration of an installation procedure using rolling supports.

4. INTERFACES

4.1 Allowed envelope

The cryostat shell ID and the shield OD need to be well matched, in particular the PS cryostat end plate ID's need to be precise and matched to the shield OD to within about 1 to 2 mm. The cryostat shell needs to have a circumference that is well matched to the shield stiffener ring circumferences, and the out of round of the cryostat shell between the end points can be maybe a few mm because it will be brought back into round during insertion.

Need detail drawings here.

4.2 Fluid

The coolant (presumably water) must pass through the vacuum closure plate at the proton beam exit side of the PS. Any couplings or gaskets between those two objects must not be subject to radiation damage failure, as the consequences of a leak of the highly radioactive coolant are severe.

5. EXPECTED PERFORMANCE

5.1 Estimated Radiation Load On PS Coils

The expected energy deposition in the PS coils due to radiation from the production target is determined using a GEANT3 [2] Monte Carlo simulation. In the simulation, approximately 10^6 8 GeV protons strike the production target (see MECO-Target-03-001 for details) inside the shield where many interact. Secondary particles, chosen randomly using known production cross-sections, are generated for each interaction within the materials of the production target, heat shield, or the PS magnet. Each particle is tracked until it interacts or decays. Energy deposition from all particles entering the volume of the PS coils is recorded to determine the local heating. The PS coils are subdivided into ten symmetric bins in azimuth for these studies. The results are scaled up to the nominal 4×10^{13} protons per second average beam intensity. The total dose in any bin in each coil is calculated from the energy deposition rate assuming a nominal MECO lifetime of 3×10^7 seconds. In Table 5.1 below, the maximum instantaneous power and total dose are calculated at the inner radial edge, where the flux is highest, by taking the average power for the highest power angular bin within a coil and applying a 35% correction to reflect the known radial dependence of the energy deposition (Figure 5.2). Additional details on the methods used and the optimization studies of the shield shape and materials can be found in [3] and [4]. These studies have recently been updated to reflect changes in the number of coils and revised radial builds for each of those coils [5]. The results of these studies using the revised PS geometry are summarized here. The table below lists the average power deposited within the PS coils, the maximum *instantaneous* (note that this is twice the average value due to the proton beam's 50% duty cycle) local heating at the inner edge of each coil and the maximum integrated dose at that point. The total coil heat load and overall maxima for local heating and dose are also listed, as are the average load in each coil's aluminum mandrel and the inner wall of the liquid helium vessel.

Table 5.1 – Summary of GEANT energy deposition simulation results

Summary of Results											
Coil	**PS01**	**PS02**	**PS03**	**PS04**	**PS05**	**PS06**	**PS07**	**PS08**	**PS09**	**PS10**	**PS11**
Average power dissipated in coil (W)	7.3	5.8	5.3	5.8	11.9	9.8	9.3	5.1	2.2	0.4	0.2
Maximum instantaneous power at inner radial edge of coil (mW/gm)	17.0	11.0	8.6	10.6	21.1	16.3	14.3	8.8	3.6	0.7	0.4
Average power dissipated in aluminum mandrel (W)	1.4	0.9	0.8	0.9	1.3	1.8	1.5	0.7	0.4	0.2	0.1
Maximum integrated lifetime dose at inner radial edge of coil (MRad)	25.5	16.5	12.9	15.9	31.7	24.4	21.4	13.2	5.4	1.1	0.6

Average total power dissipated in all PS coils	63.2 W
Average total power dissipated in all PS mandrels	10.0 W
Average total power dissipated in PS helium vessel inner wall	17.0 W
Average total power dissipated in PS Cold Mass	90.2 W
Maximum instantaneous power at inner radial edge of any coil	21.1 mW/gm
Maximum integrated dose in any coil segment	31.7 MRad or 0.317 MGy

In Figure 5.1 the distributions of deposited energy for each particle species entering the PS coil mass are shown. The vertical scale is number of interactions in each 1 MeV energy bin for approximately 10^6 primary protons on target. Figure 5.2 illustrates the radial dependence of the energy deposition within one quadrant of coil PS06.

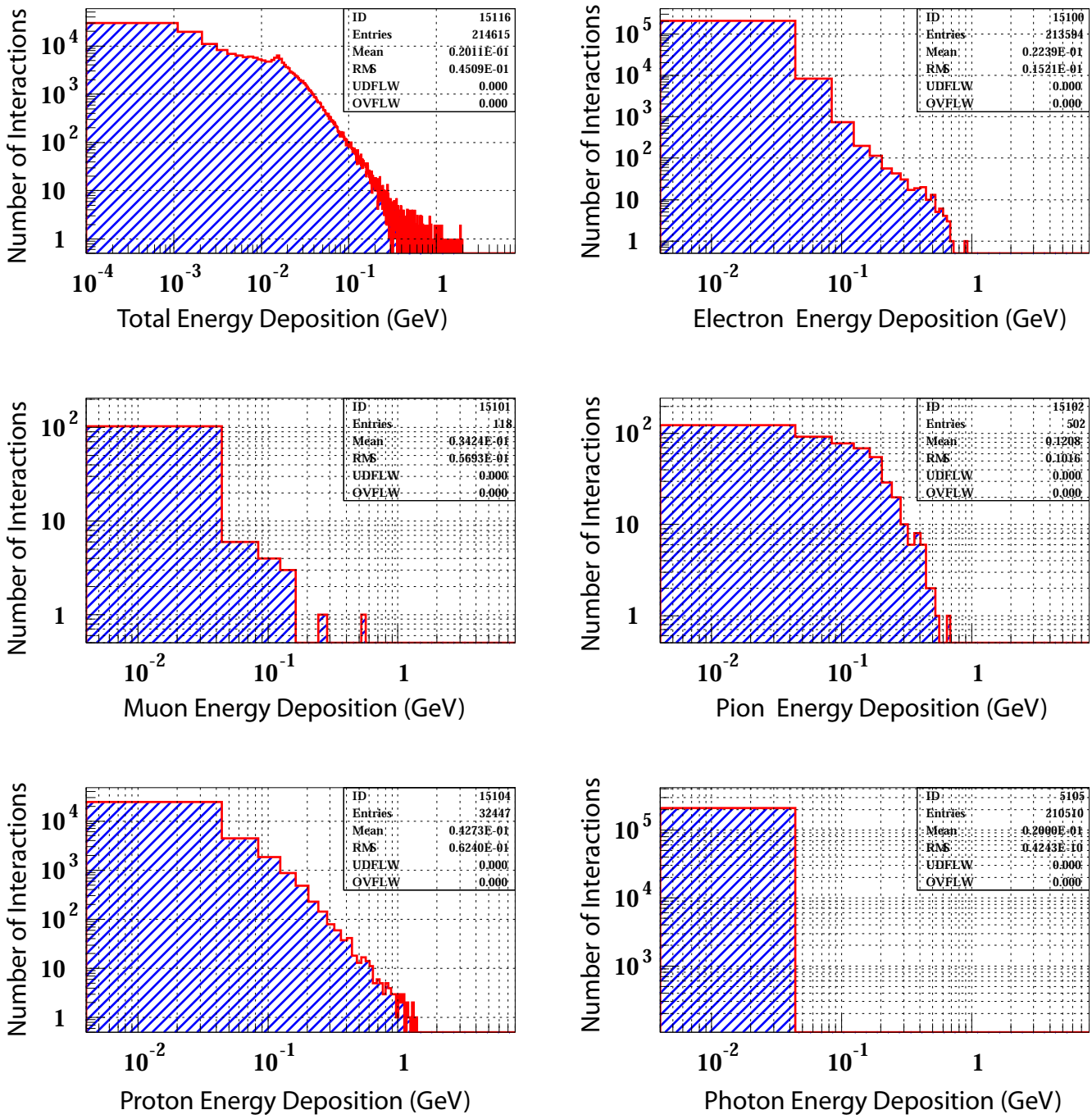

Figure 5.1 – The distribution of energy deposition within the coils for each particle species.

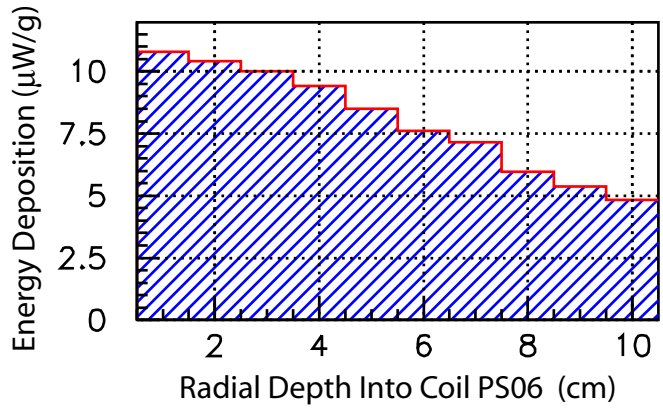

Figure 5.2 – The radial distribution of deposited energy within the highest activity quadrant of coil PS06.

Table 5.2 lists the number per unit area per second of each species of particles passing through the inner radial surface of each PS coil and the average rates for all coils. Due to limited Monte Carlo statistics, only the average rate is listed for muons. The rates are calculated using the nominal beam intensity. Table 5.3 lists the average energy for each type of radiation entering the PS coils. Note that both electrons and positron contributions are included under the "Electron" headings and similarly μ+ and μ– are included under "Muons", etc. Figure 5.3 illustrates the relative rates of each particle type entering the coils as a function of energy.

Table 5.2 – The number of particles traversing the inner radial surface of each PS coil per cm^2 per second at the nominal beam intensity.

	Electrons	Muons	Pions	Neutrons	Protons	Photons
PS01	1.3×10^6		1.6×10^5	1.2×10^9	3.5×10^5	2.0×10^8
PS02	6.4×10^5		6.5×10^4	1.0×10^9	1.7×10^5	1.6×10^8
PS03	5.4×10^5		6.5×10^4	9.5×10^9	2.8×10^5	1.6×10^8
PS04	1.1×10^6		9.1×10^4	1.1×10^9	4.9×10^5	1.8×10^8
PS05	1.2×10^6		1.8×10^5	1.5×10^9	9.0×10^5	2.7×10^8
PS06	1.8×10^6		4.5×10^5	2.2×10^9	1.4×10^6	3.9×10^8
PS07	1.7×10^6		4.3×10^5	2.0×10^9	1.2×10^6	3.2×10^8
PS08	1.4×10^6		1.4×10^5	1.6×10^9	5.9×10^5	2.6×10^8
PS09	6.4×10^5		5.8×10^4	7.9×10^8	3.5×10^5	1.2×10^8
PS10	4.1×10^5		1.1×10^4	3.1×10^8	5.8×10^4	4.3×10^7
PS11	1.5×10^5			1.6×10^8		1.9×10^7
Averages	9.7×10^5	4.26×10^3	1.5×10^5	1.1×10^9	5.3×10^5	1.9×10^8

Table 5.3 – The average energy of particles entering the PS coils in MeV.

Electrons	Muons	Pions	Neutrons	Protons	Photons
12	1000	1400	3.8	370	2.0

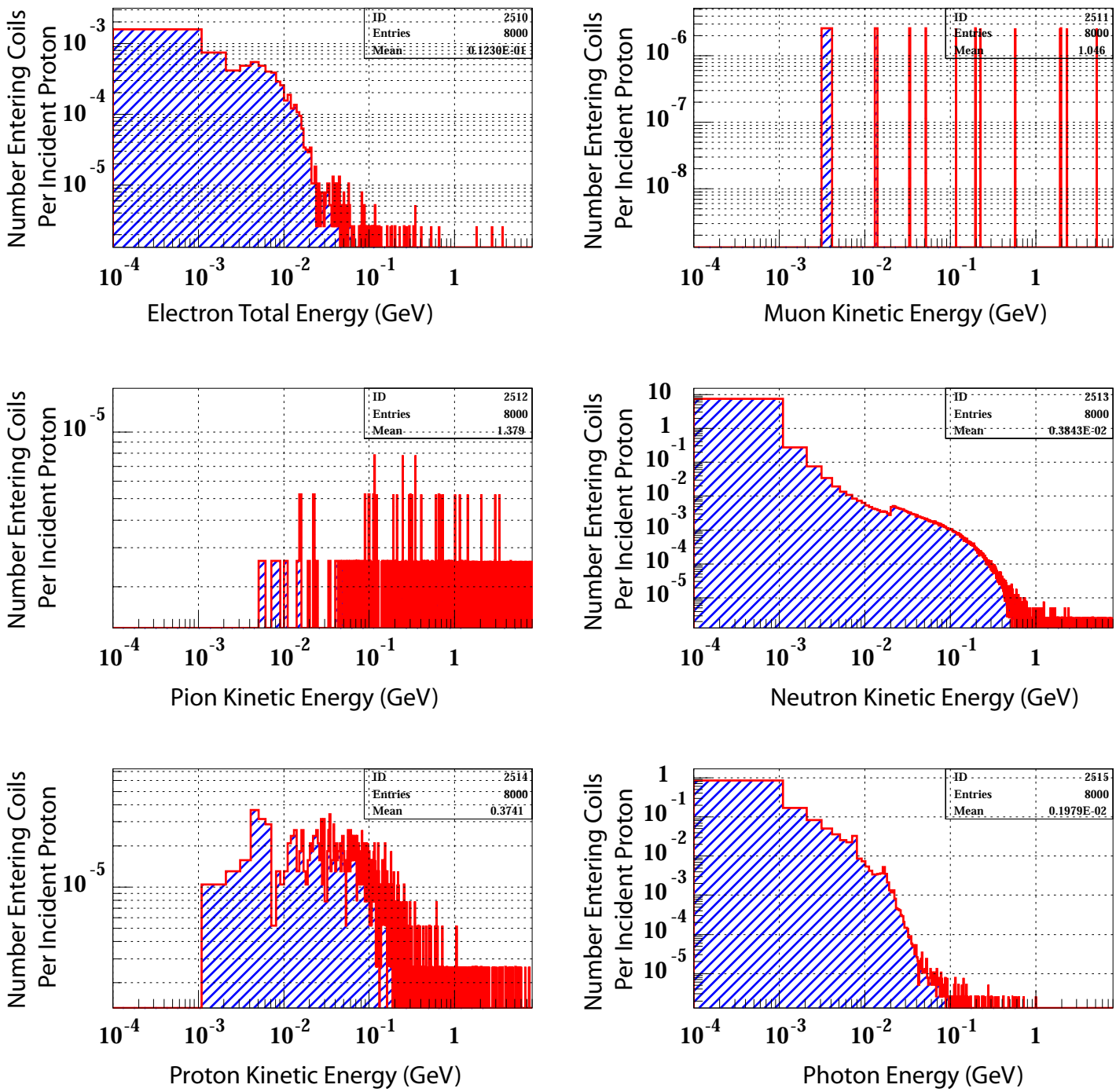

Figure 5.3 – The number of particles entering the PS coils per incident proton as a function of energy.

5.2 Expected Activation

TBD.

6. REFERENCES

1. Djilkibaev, R.M. and A.I. Mincer, *MECO Muon Yield Sensitivity to Production Solenoid Inner Bore Size*, MECO Collaboration Internal Memo **MECO073 (**2001)
2. Brun, R., et al., *Program GEANT3*, DD/EE/84-1, CERN, (1984)
3. Tumakov, V., *Energy Deposition in the Production Solenoid Cold Mass*, MECO Collaboration Internal Memo **MECO065 (**2001)
4. Tumakov, V., *Calculation of the Energy Deposition in the Coils of the Production Solenoid with a Configuration According to MIT Design*, MECO Collaboration Internal Memo **MECO070 (**2001)
5. Liu, T.J. and B. Smith, *newpscoils.xls*, 12/05/2002, Revised coil information eliminating internal cable splices.